The title: Effect of glycosylation on biodistribution of radiolabeled glucagon-like peptide 1

Ayahisa Watanabe [a, f], Ken-ichi Nishijima [c], Songji Zhao [d, e], Yoshikazu Tanaka [f], Takeshi Itoh [f], Hiroshi Takemoto [f], Nagara Tamaki [b, e] and Yuji Kuge [a-c, *]

[a] Department of Radiobiology, Graduate School of Medicine, Hokkaido University

[b] Central Institute of Isotope Science, Hokkaido University

[c] Department of Molecular Imaging, Graduate School of Medicine, Hokkaido University

[d] Department of Tracer Kinetics and Bioanalysis, Graduate School of Medicine, Hokkaido University

[e] Department of Nuclear Medicine, Graduate School of Medicine, Hokkaido University

[f] Shionogi Innovation Center for Drug Discovery, Shionogi & Co., Ltd.

[*]Corresponding author: Yuji Kuge

Address: Central Institute of Isotope Science, Hokkaido University,

Kita 15 Nishi 7, Kita-ku, Sapporo 060-0815, JAPAN

Tel: +81-11-706-7864, Fax: +81-11-706-7862, E-mail: kuge@ric.hokudai.ac.jp

Abstract

Objective Glycosylation is generally applicable as a strategy for increasing the activity of bioactive proteins. In this study, we examined the effect of glycosylation on biodistribution of radiolabeled glucagon-like peptide 1 (GLP-1) as a bioactive peptide for type 2 diabetes.

Methods Noninvasive imaging studies were performed using a gamma camera after the intravenous administration of ^{123}I-GLP-1 or ^{123}I-α2, 6-sialyl *N*-acetyllactosamine (glycosylated) GLP-1 in rats. In *ex vivo* biodistribution studies using ^{125}I-GLP-1 or ^{125}I-glycosylated GLP-1, organ samples were measured for radioactivity. Plasma samples were added to 15% trichloroacetic acid (TCA) to obtain TCA-insoluble and TCA-soluble fractions. The radioactivity in the TCA-insoluble and TCA-soluble fractions was measured.

Results In the noninvasive imaging studies, a relatively high accumulation level of ^{123}I-GLP-1 was found in the liver, which is the major organ to eliminate exogenous GLP-1. The area under the time-activity curve (AUC) of ^{123}I-glycosylated GLP-1 in the liver was significantly lower (89%) than that of ^{123}I-GLP-1. These results were consistent with those of *ex vivo* biodistribution studies using ^{125}I-labelled peptides. The AUC of ^{125}I-glycosylated GLP-1 in the TCA-insoluble fraction was significantly higher (1.7-fold) than that of GLP-1.

Conclusions This study demonstrated that glycosylation significantly decreased the distribution of radiolabeled GLP-1 into the liver and increased the concentration of

radiolabeled GLP-1 in plasma. These results suggested that glycosylation is a useful strategy for decreasing the distribution into the liver of bioactive peptides as desirable pharmaceuticals.

Keywords: noninvasive imaging, biodistribution, glycosylation, glucagon-like peptide 1

1. Introduction

Glucagon-like peptide 1 (GLP-1) is an incretin peptide hormone secreted from intestinal L-cells in response to orally taken nutrients [1]. It stimulates insulin secretion from β-cells in a glucose-dependent manner. GLP-1 also suppresses glucagon secretion, gastric emptying, and appetite and improves pancreatic β-cell functions. It is now attracting considerable attention owing to the therapeutic benefits for type 2 diabetes [1-7]. However, the use of GLP-1 as a therapeutic agent is limited by its low *in vivo* activity. Under physiological conditions, GLP-1 is rapidly eliminated by glomerular filtration [8] and hepatic extraction [5, 9]. In addition, GLP-1 is rapidly inactivated by proteolytic enzymes such as dipeptidyl peptidase IV (DPP-IV) [10-12] and neutral endopeptidase (NEP) 24.11 [13-15] in plasma.

To improve the pharmacokinetic property of GLP-1, a number of studies have been conducted. GLP-1 analogues were designed by attaching chemical groups [16] or by substituting amino acids of the peptide [17]. Moreover, conjugation with polyethylene glycol (PEG) was shown to improve the proteolytic stability of GLP-1, as well as other therapeutic peptides and proteins [18, 19]. Exendin-4, which is a GLP-1 analogue isolated from the saliva of the Gila monster *Heloderma suspectum*, has a 53% amino acid sequence identity with GLP-1 [20]. Exendin-4, which is resistant to degradation by DPP-IV [21] and NEP 24.11 [13], has a longer extended half-life and higher *in vivo* activity than GLP-1 [8, 22]. These approaches have shown

varying degrees of success. However, loss of structure or *in vitro* activity, poor efficacy, manufacturing difficulties and immunogenicity have limited their usefulness.

As another approach to developing novel analogues, glycoengineering is generally applicable as a strategy for increasing *in vivo* activity or improving the pharmacokinetic properties of proteins [23, 24]. A notable example is a glycosylated analogue of a mutated human erythropoietin with a higher plasma concentration-profile, an increased *in vivo* activity and a decreased immunogenicity [24-26]. Different from protein, no actual study using glycoengineering for increasing *in vivo* activity or improving the pharmacokinetic property of peptides has been reported, because of difficulty in synthesis of glycopeptides having homogeneous glycoforms.

Ueda *et al*. applied a glycoengineering strategy to GLP-1 [27]. They synthesized many different types of glycosylated GLP-1 using chemoenzymatic approaches and for the first time, attempted to examine the effect of glycosylation on proteolytic resistance using synthetic glycopeptides having homogeneous glycoforms. In particular, GLP-1 with α2, 6-sialyl *N*-acetyllactosamine (glycosylated GLP-1, Figure 1) showed greatly improved stability against DPP-IV and NEP 24.11 as compared with GLP-1, although both peptides showed the same affinity to the GLP-1 receptor. Moreover, glycosylated GLP-1 showed the marked blood glucose-lowering activity in diabetic *db/db* mice compared with GLP-1.

However, no actual study on the pharmacokinetics of glycosylated GLP-1 in comparison with GLP-1 has been reported. In this study, to evaluate the effects of glycosylation on the biodistribution of GLP-1, we noninvasively investigated the tissue accumulation levels of radiolabeled glycosylated GLP-1 in comparison with radiolabeled GLP-1 using a gamma camera. In addition, we measured the radioactivity in the plasma after intravenous administration of radiolabeled GLP-1 and glycosylated GLP-1.

2. Materials and methods

2.1. Radioiodination of GLP-1 and glycosylated GLP-1

GLP-1 was purchased from the Peptide Institute, Inc. Glycosylated GLP-1 was synthesized by Shionogi & Co., Ltd. as described previously [27]. GLP-1 and glycosylated GLP-1 were iodinated by the chloramine-T method, in accordance with a previously reported procedure [28] with slight modifications. In brief, $NH_4{}^{123}I$ (Nihon Medi-Physics Co., Ltd.) was added to 10 µL of 0.01 mol/L NaOH and 5.15 µg/mL NaI, evaporated to dryness and reconstituted in 20 µL of 0.4 mol/L phosphate buffer (PB), pH 7.4. The reconstituted solution was added to 200 pmol of GLP-1 or glycosylated GLP-1 in 90 µL of PB, then 11 µL of 3.8 mmol/L chloramine-T (Nacalai Tesque Inc.) in PB was added, the mixture was incubated at room temperature for 30 sec, and the reaction was stopped by adding 55 µL of 2.5 mmol/L

sodium metabisulfite (Nacalai Tesque Inc.) in PB. ^{123}I-GLP-1 or ^{123}I-glycosylated GLP-1 was purified by size-exclusion chromatography (PD-10 column, GE Healthcare UK Ltd.) using 0.2% BSA- PBS (-). The radiochemical yield was 24.5%, and the radiochemical purity was generally >90% (specific activity, ^{123}I-GLP-1: 0.200 MBq/μg of peptide, ^{123}I-glycosylated GLP-1: 0.170 MBq/μg of peptide).

Iodine labeling of GLP-1 and glycosylated GLP-1 using Na^{125}I (PerkinElmer Japan Co., Ltd.) were performed as described above. The radiochemical yield was 69.0%, and the radiochemical purity was generally >90% (specific activity, ^{125}I-GLP-1: 0.038 MBq/μg of peptide, ^{125}I-glycosylated GLP-1: 0.017 MBq/μg of peptide).

2.2. Animals

Animal care and all experimental procedures were performed with the approval of the Animal Care Committee at Hokkaido University. Male rats (Jcl:Wistar) were obtained from CLEA Japan Inc. The rats were fed a standard diet and allowed free access to water. Studies were performed using three rats per group (12 weeks of age on administration day).

2.3. Noninvasive imaging using gamma camera

Rats were anesthetized with pentobarbital (50 mg/kg of body weight,

intraperitoneally) and placed on the scanner bed in the supine position to include the entire body in the field of view. ^{123}I-GLP-1 (53.4 MBq/100 nmol (329.76 μg) of peptide/kg of body weight) or ^{123}I-glycosylated GLP-1 (75.7 MBq/100 nmol (394.02 μg) of peptide/kg of body weight) was injected into a tail vein of the rats. A dose of 100 nmol/kg was selected on the based of the pharmacological doses of GLP-1 and glycosylated GLP-1[27]. Dynamic scans (1 min x 60 frames) were performed using a gamma camera (M.CAM, Siemens Medical Solutions USA), equipped with a low-energy high-resolution parallel-hole collimator (maximum imaging field of view, 53.3 cm x 38.7 cm; spatial resolution, 3.7 mm in full-width at half-maximum). Regions of interest were set on the images to cover each organ. The results were calculated as a percent injected dose per area of organ (%ID/mm^2 of organ).

2.4. *Ex vivo* biodistribution studies

Rats anesthetized with pentobarbital were injected with ^{125}I-GLP-1 (12.7 MBq/100 nmol (329.76 μg) of peptide/kg of body weight) or ^{125}I-glycosylated GLP-1 (6.8 MBq/100 nmol (394.02 μg) of peptide/kg of body weight) into a tail vein and sacrificed 2, 15, 30 and 60 min after intravenous administration. Organs were collected, weighed and counted for radioactivity using a gamma counter (WizardTM3", PerkinElmer Japan Co., Ltd.). The results were calculated as a percent injected dose per gram of organ wet weight (%ID/g of organ).

2.5. Radioactivity in the TCA-insoluble fraction of plasma

Rats anesthetized with pentobarbital were injected with ^{125}I-GLP-1 (12.7 MBq/100 nmol of peptide/kg of body weight) or ^{125}I-glycosylated GLP-1 (6.8 MBq/100 nmol of peptide/kg of body weight) into a tail vein. Blood samples were collected 2, 5, 10, 15, 30, and 60 min after intravenous administration and centrifuged at 3000 *g* for 10 min to obtain the plasma. Fifty microliters of plasma mixed with 250 μL of 15% trichloroacetic acid (TCA) was centrifuged at 3000 *g* for 10 min. The precipitae was separated from the supernatant, and the radioactivities of the TCA-insoluble fraction (^{125}I-peptide-associated radioactivity) and the TCA-soluble fraction (free radioiodine and short fragments) were counted using a gamma counter.

2.6. Pharmacokinetic data analysis and statistical analysis

Data were represented as mean ± SD. Peak concentration (C_{max}), time to reach C_{max} (T_{max}), terminal half-life ($t_{1/2}$), area under the time-activity curve (AUC), and concentration extrapolated to time 0 (C_0) in the plasma were also calculated using WinNonlin (Professional Ver. 5.0.1, Pharsight Inc.) based on a non-compartment model with uniform weighting. Student's *t*-test was used to evaluate C_{max}, AUC and C_0. *p* values <0.05 were considered

significantly different.

3. Results

3.1. Noninvasive imaging using gamma camera

Figure 2 shows representative noninvasivly obtained images of organs following intravenous administration of ^{123}I-GLP-1 or ^{123}I-glycosylated GLP-1 to rats. Time-activity curves for organs following intravenous administration of ^{123}I-GLP-1 or ^{123}I-glycosylated GLP-1 to rats are shown in Figure 3. In the liver, the ^{123}I-GLP-1 and ^{123}I-glycosylated GLP-1 concentration increased rapidly and then declined. The AUC of ^{123}I-glycosylated GLP-1 in the liver was significantly lower (89%) than that of ^{123}I-GLP-1, and C_{max} of ^{123}I-glycosylated GLP-1 in the liver was significantly lower (73%) than that of ^{123}I-GLP-1 (Table 1). In the kidney, the ^{123}I-GLP-1 and ^{123}I-glycosylated GLP-1 concentration continued to increase for approximately 10-20 min before declined gradually. The AUC of ^{123}I-glycosylated GLP-1 in the kidney was significantly higher (1.4-fold) than that of ^{123}I-GLP-1, and the C_{max} of ^{123}I-glycosylated GLP-1 in the kidney was significantly higher (1.4-fold) than that of ^{123}I-GLP-1. In the muscle, ^{123}I-glycosylated GLP-1 accumulated similarly to ^{123}I-GLP-1.

3.2. *Ex vivo* biodistribution studies

Time-activity curves for organs following intravenous administration of ^{125}I-GLP-1 or ^{125}I-glycosylated GLP-1 to rats are shown in Figure 4. Consistent with the results of noninvasive imaging, C_{max} of ^{125}I-glycosylated GLP-1 in the liver was significantly lower (58%) than that of ^{125}I-GLP-1, and C_{max} of ^{125}I-glycosylated GLP-1 in the kidney was significantly higher (2.2-fold) than that of ^{125}I- GLP-1 (Table 2). In the muscle and pancreas, ^{125}I-glycosylated GLP-1 accumulated similarly to ^{125}I-GLP-1.

3.3. Radioactivity in the TCA-insoluble fraction of plasma

Figure 5 shows the radioactivity in the TCA-insoluble fraction of plasma after intravenous administration of ^{125}I-GLP-1 or ^{125}I-glycosylated GLP-1 to rats. The radioactivity in the TCA-insoluble fraction showed more rapid elimination in rats given ^{125}I-GLP-1, as compared with that in rats given ^{125}I-glycosylated GLP-1. The AUC was significantly higher for ^{125}I-glycosylated GLP-1 (1.7-fold) than that for ^{125}I-GLP-1, and the C_0 was significantly higher (1.4-fold) for ^{125}I-glycosylated GLP-1 than that for ^{125}I-GLP-1 (Table 3). On the other hand, there was no significant difference in the $t_{1/2}$ between the both ^{125}I-peptides. The ratios of radioactivity in the TCA-insoluble fraction to the total radioactivity in plasma were comparable between ^{125}I-GLP-1 and ^{125}I-glycosylated GLP-1 up to 10-15 min; thereafter, the ratios were lower for ^{125}I-GLP-1 than for ^{125}I-glycosylated GLP-1 (Table 4).

4. Discussion

In this study, to evaluate the effects of glycosylation on the biodistribution of GLP-1, we investigated the tissue accumulation levels of radiolabeled glycosylated GLP-1 in comparison with radiolabeled GLP-1 using a gamma camera. In our noninvasive imaging studies, a relatively high accumulation level of ^{123}I-GLP-1 was found in the liver. The AUC of ^{123}I-glycosylated GLP-1 in the liver was significantly lower (89%) than that of ^{123}I-GLP-1. These results were consistent with those of *ex vivo* biodistribution studies using ^{125}I-labelled peptides. The AUC of the radioactivity in the TCA-insoluble fraction of plasma was significantly higher in rats given ^{125}I-glycosylated GLP-1 (1.7-fold) than in rats given ^{125}I-GLP-1. This study demonstrates that glycosylation significantly decreased the distribution of radiolabeled GLP-1 into the liver and increased the concentration of radiolabeled GLP-1 in plasma.

We applied the noninvasive imaging approach to investigate the biodistribution of radiolabeled GLP-1 and glycosylated GLP-1. The AUC of ^{123}I-glycosylated GLP-1 in the liver was significantly lower than that of ^{123}I-GLP-1. It should be noted, however, that the level of the early-phase distribution (before 15 min) of ^{123}I-glycosylated GLP-1 was lower than that of ^{123}I-GLP-1, whereas the levels of late-phase distribution (after 30 min) were

similar for both peptides. As shown in Table 4, the ratios of radioactivity in the TCA-insoluble fraction to the total radioactivity in plasma for the ^{125}I-labelled peptides were comparable between ^{125}I-GLP-1 and ^{125}I-glycosylated GLP-1 up to 10-15 min, although the ratios were lower for ^{125}I-GLP-1 than for ^{125}I-glycosylated GLP-1 after 30 min (Table 4). Accordingly, it appears that glycosylation significantly inhibited the distribution of GLP-1 into the liver. As for the late-phase distribution of ^{125}I-GLP-1 and ^{125}I-glycosylated GLP-1 into the liver, however, we should take other factors, including radioactive metabolites, into consideration. Consequently, glycosylation improved the pharmaceutical properties of GLP-1, because the liver is one of the major organs to metabolize and excrete exogenous GLP-1 [5, 9], and DPP-IV is abundant in hepatocytes [31].Our results were consistent with previous reports [29, 30]. In the case of recombinant neutrophil inhibitory factor (NIF), which is a glycoprotein with a mean molecular weight of 41 kDa, an increase in the number of sialylation reduces hepatic extraction of NIF [29]. In addition, the sialic acid moiety contributes to an optimal inhibition of hepatic extraction of liposome [30]. The GLP-1 receptor is also expressed in the liver, and it was reported that GLP-1 induces glycogenesis. We confirmed the same accumulation level of both peptides in the pancreas, which is main target organ, and that the expression level of the GLP-1 receptor was higher in the pancreas than in the liver, suggesting that glycosylation does not affect the specific binding to the GLP-1 receptor. Accordingly, we do not consider

that the decrease in radioactivity in the liver is caused by the impairment of the specific binding to the GLP-1 receptor owing to glycosylation.

In contrast to the liver, the distribution of ^{123}I-glycosylated GLP-1 in the kidney was significantly higher than that of ^{123}I-GLP-1. Similarly to GLP-1, glycosylated GLP-1 seems to be filtered in the glomeruli because of the small molecular size (GLP-1, 3297.6 Da; glycosylated GLP-1, 3940.2 Da). Glycosylated GLP-1 may be more rapidly excreted by glomerular filtration compared with GLP-1, due to its higher hydrophilicity as compared with GLP-1. Although exendin-4, which is a GLP-1 analogue isolated from the saliva of the Gila monster *Heloderma suspectum*, is exclusively filtered in the glomeruli [8], its use for treatment of type 2 diabetes with once-weekly dosing is available using a long-acting release formulation, microspheres which consists of a poly (lactide-coglycolide) polymeric matrix [32]. Thus, to minimize the rapid renal loss of glycosylated GLP-1, further studies for preparing a long acting release formulation are necessary.

We counted the radioactivity of the TCA-insoluble fraction, which included ^{125}I-peptide-associated radioactivity, and that of the TCA-soluble fraction, which included free radioiodine and short fragments, using a gamma counter, and we showed the radioactivity of the TCA-insoluble fraction of the plasma as plasma radioactivity. In the TCA-insoluble fraction of the plasma, the AUC of radioactivity of ^{125}I-glycosylated GLP-1 was higher

(1.7-fold) than that of ^{125}I-GLP-1. Our results showed that glycosylation decreased the distribution of GLP-1 into the liver which has a relatively large volume of distribution in the body [33]. Therefore, the suppression of distribution into the liver by glycosylation might increase the radioactivity of TCA-insoluble fraction of the radiolabeled GLP-1 in plasma. A relatively high plasma level provides an advantage for *in vivo* activity of GLP-1, which might partly lead to the blood glucose-lowering activity of glycosylated GLP-1 in diabetic *db/db* mice [27]. However, there was no significant difference in $t_{1/2}$ between the radioactivity in the TCA-insoluble fraction of ^{125}I-GLP-1 and ^{125}I-glycosylated GLP-1 in this study. The renal clearance of glycosylated GLP-1 may also be more rapid compared with GLP-1, although the reason for this is not clear at present. Further study is necessary to clarify the mechanism. As shown by in vivo imaging, a radioiodinated peptide, probably that of free radioiodine, accumulated in the thyroid gland 60 min after administration of ^{123}I-GLP-1 but not ^{123}I-glycosylated GLP-1, suggesting that glycosylation could improve the stability of GLP-1 in the plasma. Actually, the ratios of radioactivity in the TCA-insoluble fraction to the total radioactivity in plasma were lower for ^{125}I-GLP-1 than that of ^{125}I-glycosylated GLP-1 particularly after 30 min. In the present study, however, we were unable to perform a detailed analysis of radioactive metabolites in the blood. Additional studies are required to evaluate the radioactive metabolites, in order to further understand the pharmacokinetic properties,

including metabolic profiles, of GLP-1 and glycosylated GLP-1.

In contrast to ex vivo experiments, in vivo imaging enables pharmacokinetic analysis, noninvasive quantitative evaluation of radiopharmaceuticals in individual animals, and the use of a reduced number of animals [34]. By in vivo imaging, we performed pharmacokinetic analysis and quantitative evaluation of the biodistribution of radiolabeled GLP-1 and glycosylated GLP-1 in individual animals (n=3/group) at many time points. On the other hand, ex vivo experiments (n=12/group) were supplementarily carried out at a few time points to confirm the results of in vivo imaging.

In conclusion, this study demonstrates that glycosylation significantly decreased the distribution of radiolabeled GLP-1 into the liver and increased the concentration of radiolabeled GLP-1 in plasma. Our results might partly explain the mechanism underlying the blood glucose-lowering activity of glycosylated GLP-1 in diabetic *db/db* mice. This study is the first attempt to examine the effect of glycosylation on the biodistribution of synthetic glycopeptides by noninvasive imaging. These results suggested that glycosylation is a useful strategy for decreasing the distribution into the liver of bioactive peptides as desirable pharmaceuticals.

References

1. Deacon CF. Therapeutic strategies based on glucagon-like peptide 1. Diabetes. 2004; 53: 2181–2189 .

2. Arulmozhi DK, Portha B. GLP-1 based therapy for type 2 diabetes. Eur. J. Pharm. Sci. 2006; 28: 96-108.

3. Holst JJ, Ørskov C. The incretin approach for diabetes treatment: modulation of islet hormone release by GLP-1 agonism. Diabetes. 2004; 53: S197-204.

4. Holst JJ, Deacon CF, Vilsbøll T, Krarup T, Madsbad S. Glucagon-like peptide-1, glucose homeostasis and diabetes. Trends Mol. Med. 2008; 14: 161-168.

5. Kieffer TJ, Habener JF. The glucagon-like peptides. Endocr. Rev. 1999; 20: 876–913.

6. Meier JJ, Nauck MA. Glucagon-like peptide 1 (GLP-1) in biology and pathology. Diabetes Metab. Res. Rev. 2005; 21: 91-117.

7. Nauck MA, Meier JJ. Glucagon-like peptide 1 and its derivatives in the treatment of diabetes. Regul. Pep. 2005; 128: 135-148.

8. Simonsen L, Holst JJ, Deacon CF. Exendin-4, but not glucagon-like peptide-1, is cleared exclusively by glomerular filtration in anaesthetised pigs. Diabetologia. 2006; 49: 706–712.

9. Deacon CF, Pridal L, Klarskov L, Olesen M, Holst JJ. Glucagon-like peptide 1 undergoes differential tissue-specific metabolism in the anesthetized pig. Am. J. Physiol. 1996; 271: E458-464

10. Deacon CF, Johnsen AH, Holst JJ. Degradation of glucagon-like peptide-1 by human plasma in vitro yields an N-terminally truncated peptide that is a major endogenous metabolite in vivo. J. Clin. Endocrinol. Metab. 1995; 80: 952-957.

11. Kieffer TJ, McIntosh CHS, Pederson RA. Degradation of glucose-dependent insulinotropic polypeptide and truncated glucagon-like peptide 1 in vitro and in vivo by dipeptidyl peptidase IV. Endocrinology. 1995; 136: 3585-3596.

12. Mentlein R, Gallwitz B, Schmidt WE. Dipeptidyl-peptidase IV hydrolyses gastric inhibitory polypeptide, glucagon-like peptide-1 (7-36) amide, peptide histidine methionine and is responsible for their degradation in human serum. Eur. J. Biochem. 1993; 214: 829-835.

13. Hupe-Sodmann K, McGregor GP, Bridenbaugh R, Göke R, Göke B, Thole H, et al. Characterization of the processing by human neutral endopeptidase 24.11 of GLP-1 (7-36) amide and comparison of the substrate specificity of the enzyme for other glucagon-like peptides. Regul. Pep. 1995; 58: 149-156.

14. Hupe-Sodmann K, Göke R, Göke B, Thole HH, Zimmermann B, Voigt K, et al. Endoproteolysis of glucagon-like peptide (GLP) -1 (7-36) amide by ectopeptidases in RINm5F cells. Peptides. 1997; 18: 625-632.

15. Plamboeck A, Holst JJ, Carr RD, Deacon CF. Neutral endopeptidase 24.11 and dipeptidyl peptidase IV are both mediators of the degradation of glucagon-like peptide 1 in the anaesthetised pig. Diabetologia. 2005; 48: 1882-1890.

16. O'Harte FP, Mooney MH, Lawlor A, Flatt PR. N-terminally modified glucagon-like peptide-1 (7-36) amide exhibits resistance to enzymatic degradation while maintaining its antihyperglycaemic activity in vivo. Biochim. Biophys. Acta. 2000; 1474: 13-22.

17. Deacon CF, Knudsen LB, Madsen K, Wiberg FC, Jacobsen O, Holst JJ. Dipeptidyl peptidase IV resistant analogues of glucagon-like peptide-1 which have extended metabolic stability and improved biological activity. Diabetologia. 1998; 41: 271-278.

18. Chae SY, Chun YG, Lee S, Jin CH, Lee ES, Lee KC, et al. Pharmacokinetic and pharmacodynamic evaluation of site-specific PEGylated glucagon-like peptide-1 analogs as flexible postprandial-glucose controllers. J. Pharm. Sci. 2009; 98: 1556-1567.

19. Lee SH, Lee S, Youn YS, Na DH, Chae SY, Byun Y, et al. Synthesis, characterization, and pharmacokinetic studies of PEGylated glucagon-like peptide-1. Bioconjugate Chem. 2005; 16: 377-382.

20. Göke R, Fehmann HC, Linn T, Schmidt H, Krause M, Eng J, et al. Exendin-4 is a high potency agonist and truncated exendin-(9-39)-amide an antagonist at the glucagon-like peptide 1-(7-36)-amide receptor of insulin-secreting beta-cells. J. Biol. Chem. 1993; 268: 19650-19655.

21. Thum A, Hupe-Sodmann K, Göke R, Voigt K, Göke B, McGregor GP. Endoproteolysis by isolated membrane peptidases reveal metabolic stability of glucagon-like peptide-1 analogs, exendins-3 and -4. Exp. Clin. Endocrinol. Diabetes. 2002; 110: 113-118.

22. Young AA, Gedulin BR, Bhavsar S, Bodkin N, Jodka C, Hansen B, et al. Glucose-lowering and insulin-sensitizing actions of exendin-4: studies in obese diabetic (ob/ob, db/db) mice, diabetic fatty Zucker rats, and diabetic rhesus monkeys (Macaca mulatta). Diabetes. 1999; 48: 1026-1034.

23. Sato M, Furuike T, Sadamoto R, Fujitani N, Nakahara T, Niikura K, et al. Glycoinsulins: dendritic sialyloligosaccharide-displaying insulins showing a prolonged blood-sugar-lowering activity. J. Am. Chem. Soc. 2004; 126: 14013-14022.

24. Sinclair AM, Elliott S. Glycoengineering: the effect of glycosylation on the properties of therapeutic proteins. J. Pharm. Sci. 2005; 94: 1626-1635.

25. Elliott S, Lorenzini T, Asher S, Aoki K, Brankow D, Buck L, et al. Enhancement of therapeutic protein in vivo activities through glycoengineering. Nat. Biotechnol. 2003; 21: 414-421.

26. Macdougall IC, Gray SJ, Elston O, Breen C, Jenkins B, Browne J, et al. Pharmacokinetics of novel erythropoiesis stimulating protein compared with epoetin alfa in dialysis patients. J. Am. Soc. Nephrol. 1999; 10: 2392-2395.

27. Ueda T, Tomita K, Notsu Y, Ito T, Fumoto M, Takakura T, et al. Chemoenzymatic synthesis of glycosylated glucagon-like peptide 1: effect of glycosylation on proteolytic resistance and in vivo blood glucose-lowering activity. J. Am. Chem. Soc. 2009; 131: 6237-6245.

28. Hunter R. Standardization of the chloramine-T method of protein iodination. Proc. Soc. Exp. Biol. Med. 1970; 133: 989-992.

29. Webster R, Taberner J, Edgington A, Guhan S, Varghese J, Feeney H, et al. Role of sialylation in determining the pharmacokinetics of neutrophil inhibitory factor (NIF) in the Fischer 344 rat. 1: Xenobiotica. 1999; 29: 1141-1155.

30. Gabizon A, Papahadjopoulos D. The role of surface charge and hydrophilic groups on liposome clearance in vivo. Biochim. Biophys. Acta. 1992; 10: 94-100.

31. Mentlein R. Dipeptidyl-peptidase IV (CD26)-role in the inactivation of regulatory peptides. Regul. Pept. 1999; 85: 9-24.

32. Drucker DJ, Buse JB, Taylor K, Kendall DM, Trautmann M, Zhuang D, et al. Exenatide once weekly versus twice daily for the treatment of type 2 diabetes: a randomised, open-label, non-inferiority study. Lancet. 2008; 372: 1240-1250.

33. Davies B, Morris T. Physiological parameters in laboratory animals and humans. Pharm Res. 1993; 10:1093-5

34. Melis M, Vegt E, Konijnenberg MW, de Visser M, Bijster M, Vermeij M, et al. Nephrotoxicity in mice after repeated imaging using ^{111}In-labeled peptides. J Nucl Med. 2010; 51: 973-7

Figure legends

Figure 1. Structure of glycosylated GLP-1.

Figure 2. Noninvasive imaging of rats after intravenous administration of ^{123}I-GLP-1 and ^{123}I-glycosylated GLP-1.

Red arrows indicate the liver, blue arrows indicate the kidney and brown arrows indicate the muscle.

Figure 3. Time-activity curves for liver (a), kidney (b) and muscle (c) obtained by noninvasive imaging following intravenous administration of ^{123}I-GLP-1 and ^{123}I-glycosylated GLP-1.

Open and closed circles indicate the data for ^{123}I-GLP-1 and ^{123}I-glycosylated GLP-1. Data represent mean ± SD (n=3).

Figure 4. Radioactivity in liver (a), kidney (b), muscle (c), and pancreas (d) obtained by *ex vivo* counting following intravenous administration of ^{125}I-GLP-1 and ^{125}I-glycosylated GLP-1.

Open and closed circles indicate the data for ^{125}I-GLP-1 and ^{125}I-glycosylated GLP-1. Data represent mean ± SD (n=3).

Figure 5. The radioactivity in the TCA-insoluble fraction of the plasma after intravenous administration of ^{125}I-GLP-1 and ^{125}I-glycosylated GLP-1.

Open and closed circles indicate the data for ^{125}I-GLP-1 and ^{125}I-glycosylated GLP-1. Data represent mean ± SD (n=3).

Table 1. Pharmacokinetic parameters of radioactivity in organs obtained by noninvasive imaging following intravenous administration of ^{123}I-GLP-1 or ^{123}I-glycosylated GLP-1

Parameter	^{123}I-GLP-1	^{123}I-glycosylated GLP-1
Liver		
AUC_{last} (%ID/mm^2 of organ·min/L)	0.860 ± 0.032	0.763 ± 0.016*
C_{max} (%ID/mm^2 of organ)	0.0270 ± 0.0017	0.0197 ± 0.0006*
T_{max} (min)	2.00 ± 0.00	2.00 ± 0.00
Kidney		
AUC_{last} (%ID/mm^2 of organ·min/L)	1.01 ± 0.11	1.46 ± 0.05*
C_{max} (%ID/mm^2 of organ)	0.0213 ± 0.0021	0.0297 ± 0.0021*
T_{max} (min)	11.7 ± 1.2	17.0 ± 3.5

Data represent mean ± SD (n=3).

C_{max}: peak concentration.

AUC_{last}: area under the time-activity curve.

T_{max}: time to reach C_{max}.

* $p<0.05$ by Student's *t*-test, indicates a significant difference between ^{123}I-GLP-1 and ^{123}I-glycosylated GLP-1.

Table 2. Pharmacokinetic parameters of radioactivity in organs obtained by *ex vivo* counting following intravenous administration of ^{125}I-GLP-1 or ^{125}I-glycosylated GLP-1

Parameter	^{125}I-GLP-1	^{125}I-glycosylated GLP-1
Liver		
C_{max} (%ID/g of organ)	1.95 ± 0.27	1.14 ± 0.06*
Kidney		
C_{max} (%ID/g of organ)	5.22 ± 0.08	11.7 ± 0.5**

Data represent mean ± SD (n=3).

C_{max}: peak concentration.

* $p<0.05$ by Student's *t*-test, indicates a significant difference between ^{125}I-GLP-1 and ^{125}I-glycosylated GLP-1.

** $p<0.001$ by Student's *t*-test, indicates a significant between ^{125}I-GLP-1 and ^{125}I-glycosylated GLP-1.

Table 3. Pharmacokinetic parameters of the radioactivity in the TCA-insoluble fraction of plasma following intravenous administration of ^{125}I-GLP-1 and ^{125}I-glycosylated GLP-1

Parameter	^{125}I-GLP-1	^{125}I-Glycosylated GLP-1
AUC_{last} (nmol eq.·min/L)	42337 ± 1418	71158 ± 4668*
C_0 (nmol eq./L)	2321 ± 132	3353 ± 67*
$t_{1/2}$ (min)	37.1 ± 4.5	37.8 ± 2.0

Data represent mean ± SD (n=3).

C_0: concentration extrapolated to time 0.

AUC_{last}: area under the time-activity curve.

$t_{1/2}$: terminal half-life.

* p<0.001 by Student's t-test, indicates a significant difference between ^{125}I-GLP-1 and ^{125}I-glycosylated GLP-1.

Table 4. Ratios of radioactivity ratios in TCA-insoluble fraction to total radioactivity in plasma following intravenous administration of ^{125}I-GLP-1 and ^{125}I-glycosylated GLP-1

Time (min)	^{125}I-GLP-1	^{125}I-Glycosylated GLP-1
2	96 ± 1	97 ± 1
5	92 ± 1	95 ± 2
10	85 ± 3	93 ± 2
15	73 ± 5	90 ± 1
30	37 ± 5	78 ± 3
60	22 ± 3	59 ± 4

Data represent mean ± SD (n=3).

GLP-1

HAEGT FTSDV SSYLE GQAAK EFIAW LVKG R -NH_2
7 34 36

R_1
NH

Glycosylated GLP-1

HAEGT FTSDV SSYLE GQAAK EFIAW LVNG R -NH_2
7 34 36

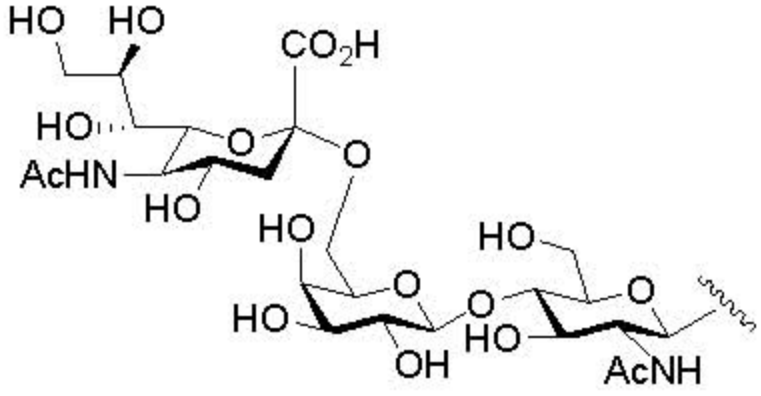

R_1: α2, 6-sialyl *N*-acetyllactosamine

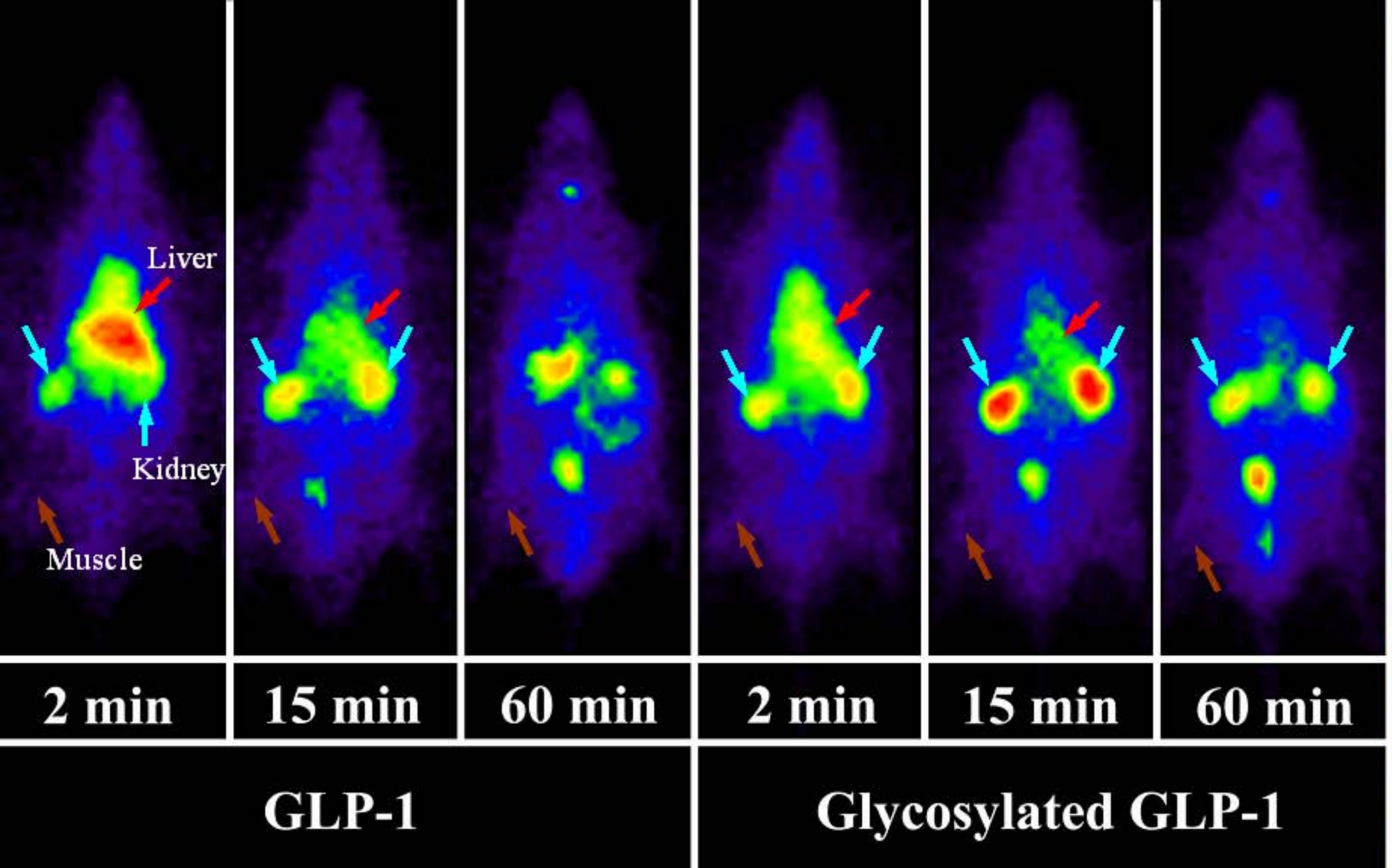
Liver
Kidney
Muscle
2 min
15 min
60 min
2 min
15 min
60 min
GLP-1
Glycosylated GLP-1

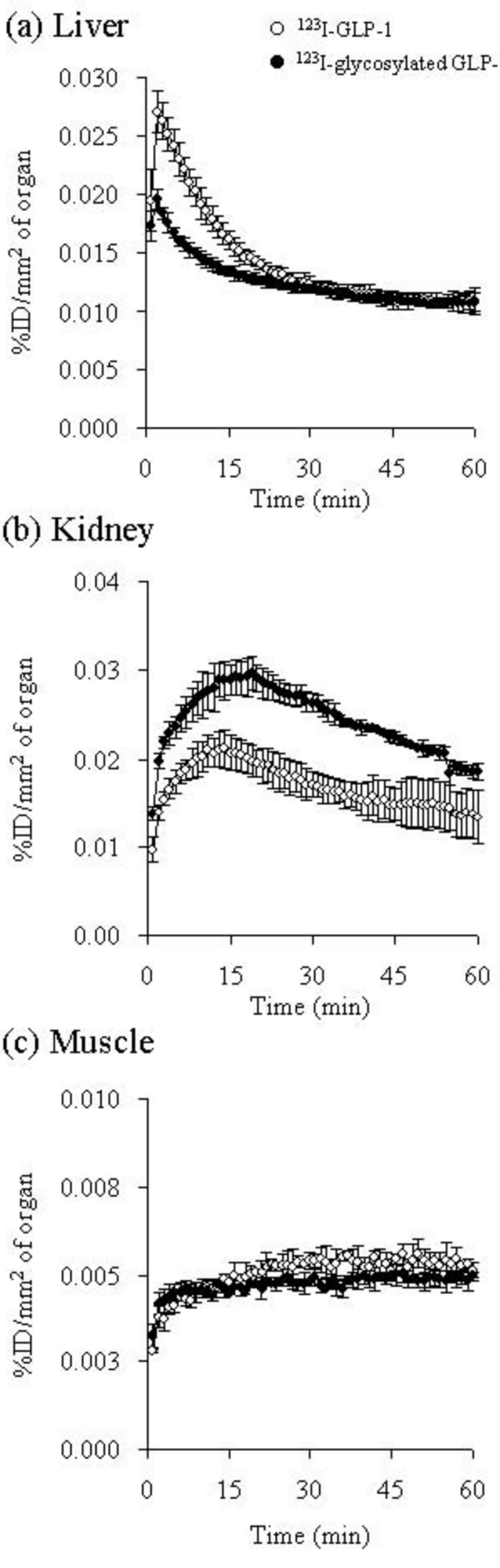
(a) Liver
○ 123I-GLP-1
● 123I-glycosylated GLP-1
0.030
0.025
0.020
0.015
0.010
0.005
0.000
%ID/mm2 of organ
0
15
30
45
60
Time (min)
(b) Kidney
0.04
0.03
0.02
0.01
0.00
%ID/mm2 of organ
0
15
30
45
60
Time (min)
(c) Muscle
0.010
0.008
0.005
0.003
0.000
%ID/mm2 of organ
0
15
30
45
60
Time (min)

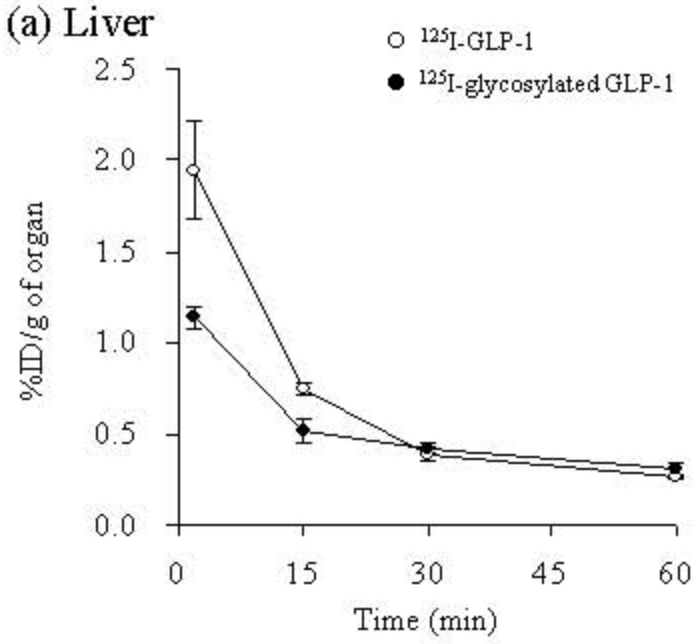
(a) Liver
125I-GLP-1
125I-glycosylated GLP-1
%ID/g of organ
Time (min)
0.0
0.5
1.0
1.5
2.0
2.5
0
15
30
45
60

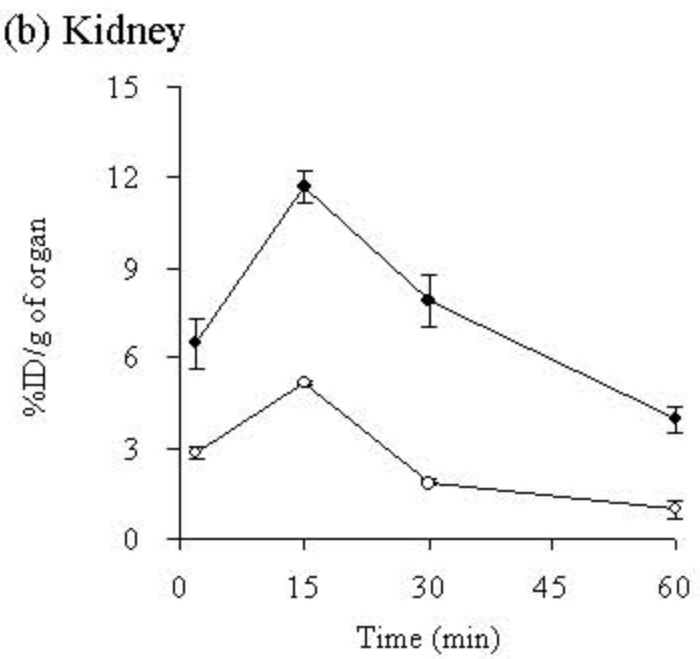
(b) Kidney
%ID/g of organ
Time (min)
0
3
6
9
12
15
0
15
30
45
60

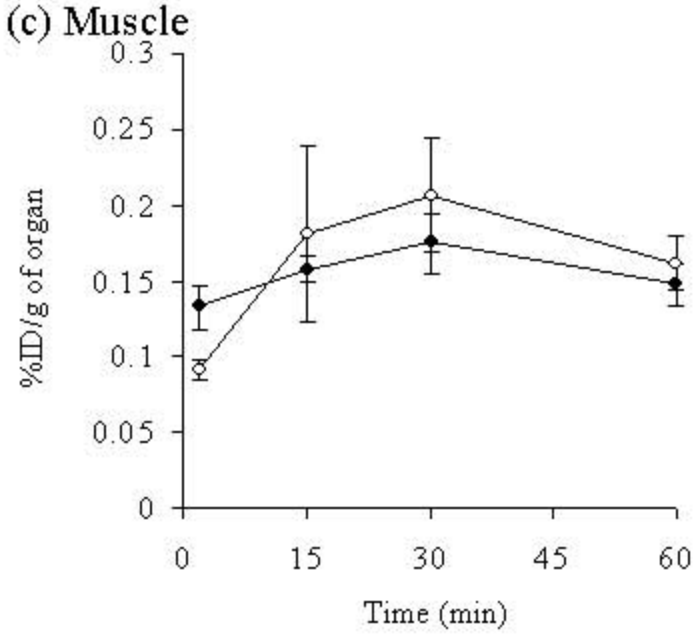
(c) Muscle
%ID/g of organ
Time (min)
0
0.05
0.1
0.15
0.2
0.25
0.3
0
15
30
45
60

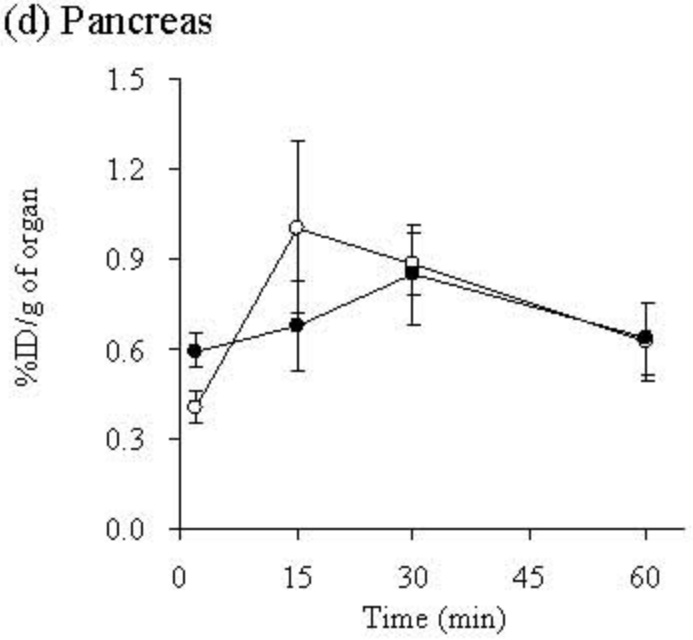
(d) Pancreas
%ID/g of organ
Time (min)
0.0
0.3
0.6
0.9
1.2
1.5
0
15
30
45
60

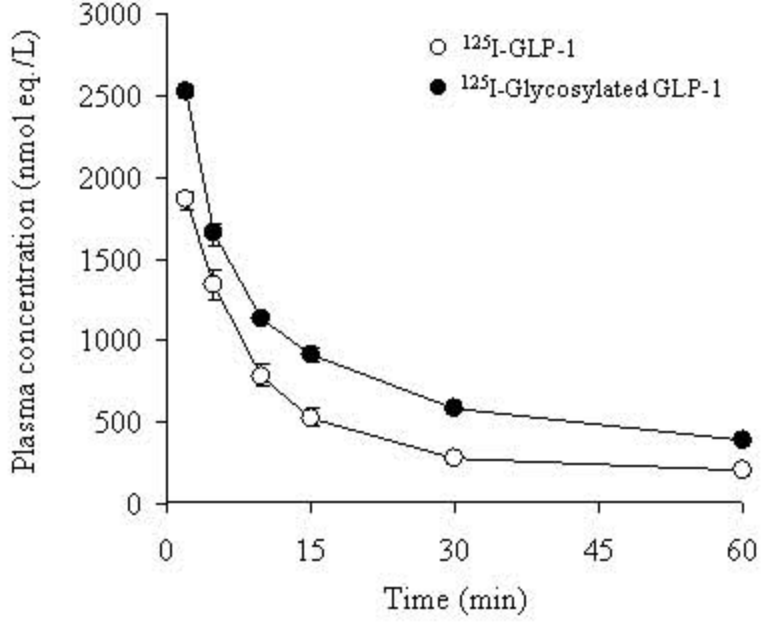
3000
2500
2000
1500
1000
500
0
Plasma concentration (nmol eq./L)
125I-GLP-1
125I-Glycosylated GLP-1
0
15
30
45
60
Time (min)